


Article

Equivalent Circuit Parameter Calculations and Characteristics Analysis of 2-DoF Direct Drive Induction Motor with a Slotted Solid Rotor

Haichao Feng ¹, Jikai Si ^{2,*} , Wei Wu ¹, Lianghui Dong ² and Zhiping Cheng ²

¹ School of Electrical Engineering and Automation, Henan Polytechnic University, Jiaozuo 454000, China; fhc@hpu.edu.cn (H.F.); wuwei1039@126.com (W.W.)

² College of Electric Engineering, Zheng Zhou University, Zhengzhou 450001, China; dlh@zzu.edu.cn (L.D.); zpcheng@zzu.edu.cn (Z.C.)

* Correspondence: sijikai527@126.com; Tel.: +86-135-2320-1034

Received: 24 March 2019; Accepted: 27 May 2019; Published: 29 May 2019



Abstract: In this paper, a modified equivalent circuit model (ECM), which considers the effects of an arc-shaped stator structure and saturation, is presented to calculate the characteristics of a two-degree-of-freedom direct drive induction motor (2DoFDDIM). The motor has a novel slotted solid rotor (SSR), which is slotted along the axial and circumferential directions, and copper is cast in the slots. The SSR is equivalent to a cage rotor by analyzing the current distribution using the circuit diagram. The corrected ECM parameter expressions of a cage rotor are proposed to calculate the SSR parameters. The characteristics obtained by ECM and finite element method are compared to verify the accuracy of the modified ECM. This paper provides reference for calculating the parameters of the induction motor with SSR.

Keywords: characteristics calculation; equivalent circuit model (ECM); finite element method; two-degree-of-freedom direct drive induction motor (2DoFDDIM)

1. Introductions

Two-degree-of-freedom motors, which produce rotary, linear and helical motions, are widely applied in the industrial fields of robots and automobiles. A two-degree-of-freedom direct drive induction motor (2DoFDDIM) consists of a rotary armature, linear armature, and solid rotor coated with a thin copper layer [1–5] and has the advantages of a simple structure and high mechanical integration. However, this motor has the disadvantages of high rotor loss and low efficiency. Slotting on the solid rotor surface is an effective method for reducing the rotor loss.

For the slotted solid rotor, the rotor core is part of the magnetic and current paths. The magnetic field distribution and equivalent circuit parameters of the solid rotor motor are difficult to calculate accurately. Numerous studies have been conducted on an induction motor with a slotted rotor. In Ref. [6], time-stepping finite element method (FEM) was used to design and analyze a solid rotor induction motor (SRIM) with skewed slits in radial and axial directions. FEM needs a long computing time. Furthermore, the physical interpretations of field quantities are indefinite. In Ref. [7], a 2D analytical method was proposed to achieve the equivalent circuit parameters of slit SRIMs. In Ref. [8], a bar-crossed rotor was presented and applied to a 2DoF induction motor, but the motor characteristics were not analyzed. In Ref. [9], a novel slotted solid rotor (SSR), which is slotted along the axial and circumferential direction on a smooth solid mover surface first and copper is cast in the slots was applied to the 2DoFDDIM, and the characteristics were analyzed through FEM. However, the equivalent circuit model (ECM) was not provided. Thus, this study aims to establish the ECM of the 2DoFDDIM to calculate the motor characteristics easily.

In this work, first, the structure and parameters are provided. Second, the SSR is equivalent to the cage rotor by analyzing the current distribution. Third, an ECM of 2DoFDDIM with SSR is established, and the characteristics are calculated. Finally, the computed and FEM simulation results are compared to verify the accuracy of the ECM.

2. Structure and Parameters

The studied 2DoFDDIM consists of two arc-shaped stators of the rotary and linear parts and a SSR, as shown in Figure 1. The motor adopts full-pitched windings. The number of parallel branches is 1. Table 1 lists the structure parameters of the motor. The feature is the rotary motion stator is just a half of the traditional stator, as shown in Figure 1a; the circumferential radian is listed in Table 1.

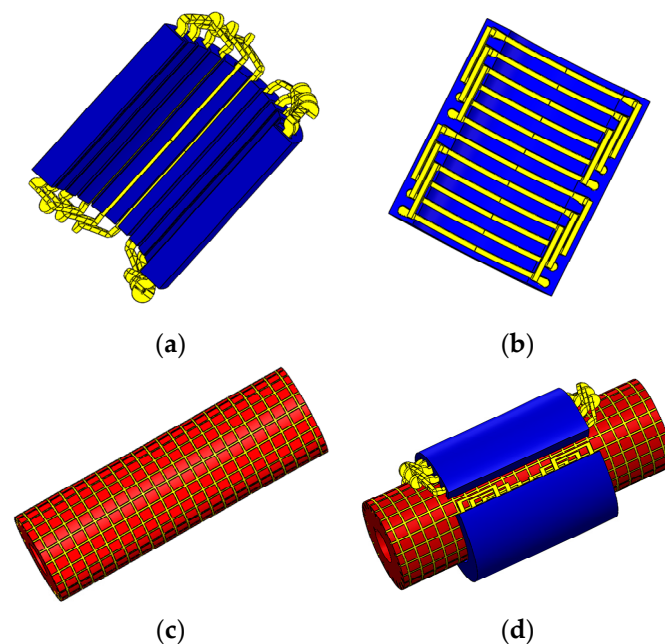


Figure 1. Structure of 2DoFDDIM: (a) Rotary motion arc-shaped armature; (b) Linear motion arc-shaped armature; (c) SSR; (d) Assembly of the 2DoFDDIM.

Table 1. Structure Parameters of 2DoFDDIM.

Item	Values/Dimension	
	Rotary Part	Linear Part
Rated voltage U_1 (V)	180	180
Supply frequency f_1 (Hz)	50	50
Pole pair p	2	2
Stator inner diameter D_{si} (mm)	98	98
Stator outer diameter D_{so} (mm)	155	155
Stator axial diameter l_{ef} (mm)	156	156
Air-gap thickness δ (mm)	2	2
Number of slots	12	12
Phase number	3	3
Number of slots per pole per phase	2	2
Number of turns per slot N	90	90
Winding diameter d_w (mm)	0.54	0.54
Circumferential radian ($^\circ$)	180	140

The SSR is shown in Figure 2. It can be known that a hollow steel cylinder is slotted along the axial and circumferential directions, and copper is cast in the slots. For the rotary part, the axial slots provide a path for the induced current caused by a rotating magnetic field. The induced current is

closed through the circumferential slots at the end. For the linear part, the roles of the axial slot and the circumferential slot are interchangeable. The shape, width, and depth of the axial slots are the same as the circumferential slots. Table 2 presents the SSR parameters.

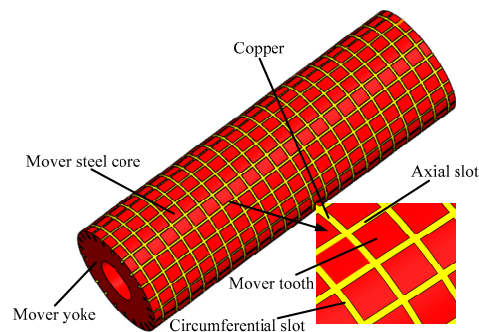


Figure 2. Structure of SSR.

Table 2. Parameters of SSR.

Items	Parameters
Rotor outer diameter D_{ro} (mm)	94
Rotor axial length L_r (mm)	600
Slot width w (mm)	2
Slot depth d (mm)	7
Slot pitch L (mm)	10.84 (axial) 11.57 (circumferential)

3. Equivalent Circuit Parameters Calculation (Rotary Part)

For the 2DoFDDIM, intricate electromagnetic field-related phenomena occur, such as the coupling effect when rotary and linear motions are considered. When the coupling effect is ignored, it can be analyzed from the perspective of a single-degree-of-freedom motor [2].

3.1. Circuit Diagram and Currents Distribution in SSR

To analyze the current distribution in SSR, the circuit diagram is obtained by using the lumped parameter method, as shown in Figure 3 [10].

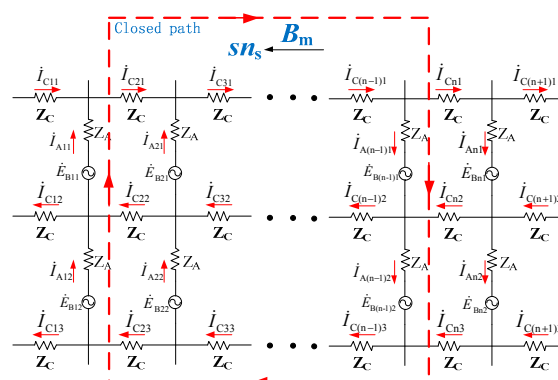


Figure 3. Circuit diagram of SSR.

In Figure 3, Z_A and Z_C are the impedances of axial and circumferential slots, respectively. I_{Am} and I_{Cm} denote the currents in axial and circumferential slots, respectively. For the rotary part of

2DoFDDIM, in the circumferential slot between the two neighboring teeth in the axial direction, the induction current density is expressed by Ref. [9].

$$J_c = \frac{1}{A_s R} \int_s \frac{\partial(B_1 - B_2)}{\partial t} dS \quad (1)$$

where A_s expresses the sectional area of the circumferential slot, R is the resistance of the copper around a tooth, S represents the superficial area of a tooth, and B_1 and B_2 refer to the magnetic flux densities through the two teeth, respectively. At the magnetic field boundary, $B_1 \neq B_2$, $J_c \neq 0$. Due to the fact that B is constant along the axial slot in the active area, i.e., $B_1 = B_2$, hence $J_c = 0$. The induced current in axial slots $I_{Am1} = I_{Amn}$ can be concluded also. Therefore, the circuit diagram of SSR is simplified, as shown in Figure 4.

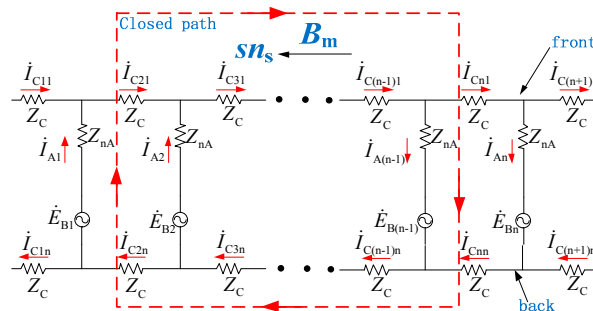


Figure 4. Simplified circuit diagram of SSR.

In Figure 4, $Z_{na} = nZ_A$ represents the sum of effective axial leakage impedance, and n is the number of effective axial slots. The simplified circuit diagram corresponds to the cage rotors. Therefore, SSR can be equivalent to a cage rotor to calculate the ECM parameters.

3.2. Equivalent Circuit

The induction motor steady-state characteristics can be easily computed using the single-phase equivalent circuit [11,12]. On the basis of Section 3, SSR can be equivalent to a cage rotor. Figure 5 shows the single-phase equivalent circuit of the rotary part of the 2DoFDDIM. R_1 , R_m , R'_{2s} and X_1 , X_m , $X'_{2\sigma}$ indicate the resistance and reactance of the primary winding, excitation, and rotor, respectively.

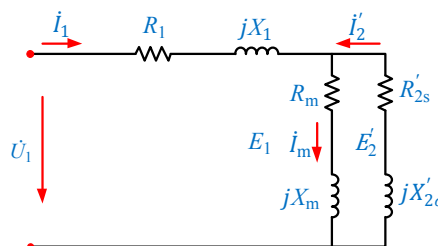


Figure 5. Single phase equivalent circuit of the rotary part.

3.3. Rotor Parameters Calculation

To simplify the calculation, the following assumptions are proposed:

- (1) The motor is supplied with balanced three-phase sinusoidal currents. The air gap flux density is constant in the axial direction.
- (2) The material primary core is isotropic, the permeability is infinite, and the conductivity is equal to zero.
- (3) The hysteresis, end, and saturation effects are ignored. The magnetic leakage in the rotor slots is neglected.

- (4) Each field includes a fundamental component, and the time curves of each field are sinusoidal.

The rotor is symmetrical in structure, and the air gap magnetic field is sinusoidal in the circumferential direction. The amplitudes of currents in the two adjacent axial slots are equal, and the electric angles differ by α_2 in phase,

$$\alpha_2 = \frac{p \times 360^\circ}{Q_2} \quad (2)$$

Q_2 is the number of axis slots under the magnetic field.

By combining Kirchhoff's current law and Figure 4, the relationship between axial and circumferential currents is $\dot{I}_{A1} = \dot{I}_{C11} - \dot{I}_{C12}$, $\dot{I}_{A2} = \dot{I}_{C12} - \dot{I}_{C13}$, \dots , and Figure 6 shows the vector diagram of currents [13,14].

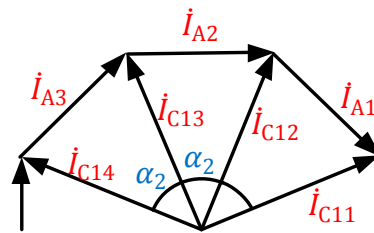


Figure 6. Vector diagram of currents.

The relationship between axial current I_A and circumferential current I_C is as follows

$$I_A = 2I_C \sin\left(\frac{\alpha_2}{2}\right) \quad (3)$$

Thus, the total losses in one axial slot and the corresponding front and back end slots are calculated by

$$P_{Cu(A+C)} = I_A^2 R_{2A} + 2I_C^2 R_C = I_A^2 \left(R_{2A} + \frac{R_C}{2 \sin^2 \frac{\alpha_2}{2}} \right) = I_A^2 R_2 \quad (4)$$

where $R_{2A} = nR_A$ is the sum of axial resistance. $R_{2(A+C)}$ is the equivalent axial resistance, when the front and back end circumferential slots are incorporated in axial slots.

$$R_{2(A+C)} = \left[nR_A + \frac{R_C}{2 \sin^2(\alpha_2/2)} \right] \quad (5)$$

The equivalent axial reactance is calculated as follows:

$$X_{2(A+C)} = \left[nX_A + \frac{X_C}{2 \sin^2(\alpha_2/2)} \right] \quad (6)$$

The expressions of the resistance and reactance of each slot are as follows:

$$\left. \begin{aligned} R_2 &= \frac{\rho L}{A} = \frac{\rho L}{dw} \\ X_2 &= 2\pi f \mu_0 \frac{N^2}{pq} L \sum \lambda \end{aligned} \right\} \quad (7)$$

where ρ is the resistivity and A is the sectional area of each slot. The $\mu_0 = 4\pi \times 10^{-7} H/m$ indicates the air permeability. N is the winding turns. The q represents the number of slots per pole per phase. $\sum \lambda$ is the sum of each slot leakage permeance.

For cage rotors, the rotor phase number $m_2 = Q_A$, Q_A refers to the rotor axial slot number, the rotor turns $N_2 = 1/2$, $K_{dp2} = 1$ represents the rotor fundamental winding and conversion coefficients

$$K = \frac{m_1}{m_2} \left(\frac{N_1 K_{dp1}}{N_2 K_{dp2}} \right)^2 = \frac{4m_1 (N_1 K_{dp1})^2}{Q_A} \quad (8)$$

where m_1 is the stator phase, N_1 denotes the number of stator conductors in the series per phase, and k_{dp1} stands for the stator fundamental winding coefficient. For conventional motors, the expressions of the equivalent rotor resistance and reactance are as follows,

$$\left. \begin{aligned} R'_{2s} &= \frac{K}{s} R_2 = \frac{4m_1 (N_1 K_{dp1})^2}{s Q_A} R_2 \\ X'_{2s} &= K X_2 = \frac{4m_1 (N_1 K_{dp1})^2}{Q_A} X_2 \end{aligned} \right\} \quad (9)$$

The ECM of the motor with a-parallel windings is as shown in Figure 7.

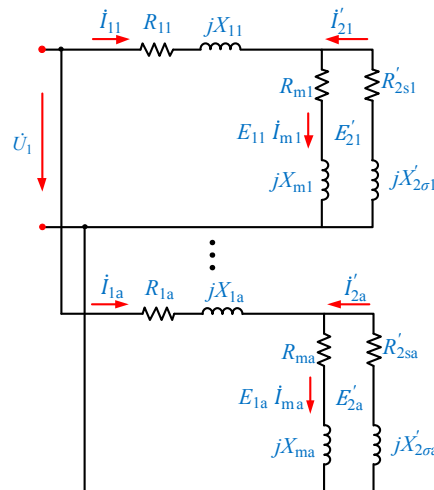


Figure 7. ECM of motors with a-parallel windings.

The expressions of the equivalent rotor resistance and reactance in each branch are

$$\left. \begin{aligned} R'_{2sn} &= a R'_{2s} = \frac{aK}{s} R_2 \\ X'_{2sn} &= a X'_{2s} = a K X_2 \end{aligned} \right\} \quad (10)$$

where $1 \leq n \leq a$. Thus, for the 2DoFDDIM, a correction coefficient $k = a = 2$ is imported to consider the influence of the arc-shaped stator structure; the expressions of the equivalent rotor resistance and reactance in Figure 5 are as follows:

$$\left. \begin{aligned} R'_{2s} &= \frac{kK}{s} R_2 = \frac{8m_1 (N_1 K_{dp1})^2}{s Q_A} R_2 \\ X'_{2s} &= k K X_2 = \frac{8m_1 (N_1 K_{dp1})^2}{Q_A} X_2 \end{aligned} \right\} \quad (11)$$

3.4. Excitation Reactance Calculation

Conventional induction motors have a small air gap. The relationship between excitation impedance calculation and equivalent rotor impedance is $Z_m \gg Z'_{2s}$, when the motor operates. Thus, Z_m is assumed to be infinite. For the studied motor, the air gap is large, and Z_m decreases. The excitation impedance is generally considered to be approximately equal to the excitation reactance, $Z_m \approx X_m$. No expression is involved to calculate the excitation reactance of an induction motor with

SSR. On the basis of the calculation of multilayer rotor induction motor [15], the expression of its excitation reactance is assumed as

$$X_m = 4f\mu_0 \frac{m_1}{\pi} \frac{(N_1 K_{dp1})^2}{p} l_{ef} \frac{\tau}{\sum \delta} \quad (12)$$

where $\sum \delta = \delta_{ef} + \delta'$ is the equivalent air gap considering the saturation of the rotor core, $\delta_{ef} = K_{c1}\delta$; $K_{c1} = \frac{t_1(4.4\delta + 0.75b_1)}{t_1(4.4\delta + 0.75b_1) - b_1^2}$ is the air-gap coefficient of the stator; t_1 is the width of the stator teeth; b_1 is the slot width of the stator slot, and δ is the length of the air gap. $\delta' = \Delta/\mu_{Fe}$ is the additional air gap, $\Delta = \sqrt{\frac{1}{\pi s f_1 \delta_{Fe} \mu_{Fe} \mu_0}}$ is the depth of penetration, and μ_{Fe} is the rotor core relative permeability. μ_{Fe} is determined by the magnetic density of the rotor core.

3.5. Equivalent Circuit Establishment

The establishment process of ECM is listed as follows, and Figure 8 shows the computational program diagram.

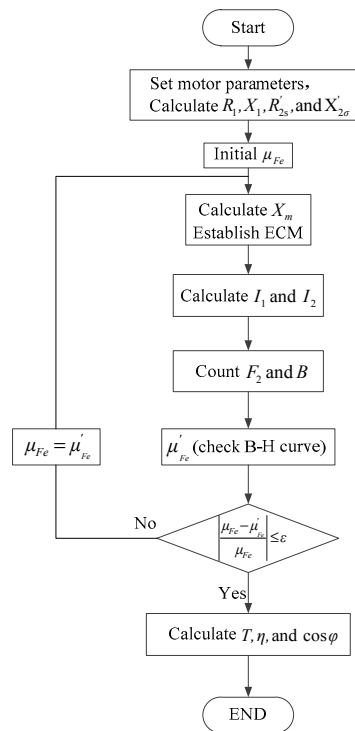


Figure 8. Computational program diagram of ECM.

- (1) Calculate the resistance and reactance of the stator and rotor.
- (2) Assume the initial relative permeability of the rotor core $\mu_{Fe} = \lim_{H \rightarrow 0} \frac{B}{H\mu_0}$, and calculate the excitation.
- (3) On the basis of the above calculation result, the initial ECM is established.
- (4) Compute the stator phase current I_1 and the excitation current I_m .
- (5) Count the amplitude of air-gap magneto motive force ($F_m = \frac{m_1}{2} \times 0.9 \frac{N_1 k_{w1} I_m}{p}$) and the air-gap flux $\Phi_g = \frac{2\mu_0}{\pi\delta} F_m \tau l_{ef}$.
- (6) Calculate the magnetic field density $B_{Fe} = \frac{2p\Phi_g}{\pi(D_{st}-2\delta)l_{ef}} \frac{(L_a+d)(L_c+d)}{L_a L_c}$ and obtain the relative permeability μ'_{Fe} corresponding to B_{Fe} by checking the B - H curve.

(7) Calculate the error. If $\left| \frac{\mu_{Fe} - \mu'_{Fe}}{\mu_{Fe}} \right| > \varepsilon$, $\mu_{Fe} = \mu'_{Fe}$, return to step (3). Otherwise, proceed to the following steps.

(8) Calculate other characteristics (i.e., output torque, efficiency, and power factor).

3.6. Equivalent Circuit Parameter Calculation Results

According to the above expressions, the excitation reactance, equivalent rotor resistance and reactance in Figure 5 can be computed. The stator resistance and reactance can be obtained by the following expressions [15].

$$\left. \begin{aligned} R_1 &= \rho \frac{l}{A_o} \\ X_1 &= 4\pi f \mu_0 \frac{N^2}{pq} l_{ef} \sum \lambda \\ \sum \lambda &= \lambda_s + \lambda_\delta + \lambda_i + \lambda_E \end{aligned} \right\} \quad (13)$$

where l is the length of a winding conductor and A_o is the conductor section. λ_s , λ_δ , λ_i , and λ_E are stator slot leakage reactance, harmonic leakage reactance, teeth leakage reactance, and end-winding leakage reactance, respectively. The computed results of the equivalent circuit parameters are shown in Figure 9.

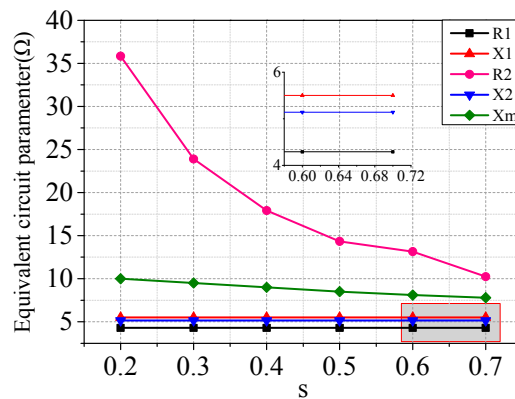


Figure 9. Computed results of equivalent circuit parameters.

Figure 9 shows that the stator resistance, stator reactance and equivalent rotor reactance are constants. The equivalent rotor resistance and excitation reactance decrease with the increasing slip, and the excitation reactance is less than the equivalent rotor resistance.

4. 3D Finite Element Analysis (Rotary Part)

Figure 10 shows the 3D FEM model of the rotary part on the basis of the stator parameters listed in Table 1 and rotor parameters listed in Table 2. Figure 11 presents the magnetic field and eddy current distributions when Slip = 1.

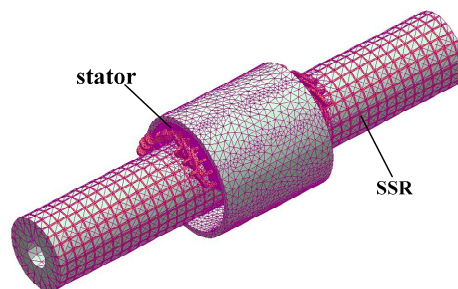


Figure 10. 3D FEM model of rotary part.

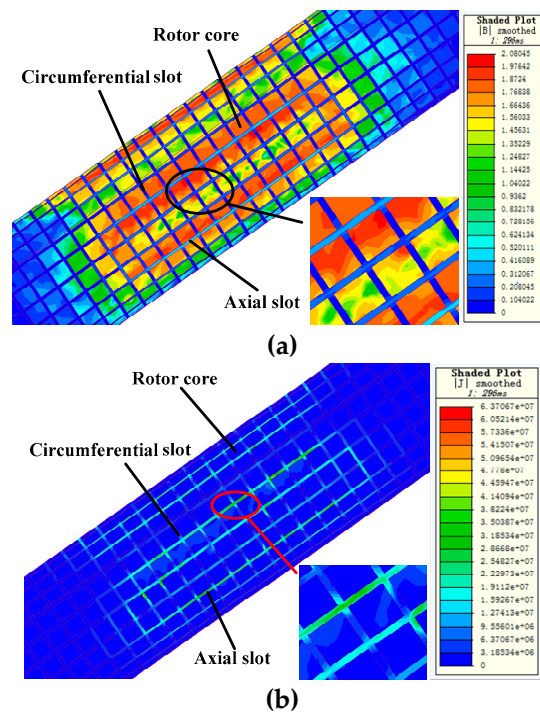


Figure 11. Magnetic field and eddy current field distributions: (a) Magnetic field; (b) Eddy current field.

Figure 11a illustrates that the magnetic field passes through the rotor teeth and yoke, and the leakage flux in slots is rarely enough to be neglected. Figure 11b exhibits that the eddy current field is almost concentrated in the axial slots. A minimal induction current is observed in the circumferential slot and rotor core. The SSR equivalent to a cage rotor is verified.

5. Results Comparison and Characteristics Analysis

5.1. The Rotary Part

The motor characteristics of the rotary part are calculated on the basis of the ECM, i.e., stator phase current, output torque, efficiency, and power factor. According to ohm's law and the physical meaning of the motor performances, the characteristics can be obtained by the following expressions [10].

- (1) Stator phase current:

$$\left. \begin{aligned} I_1 &= \frac{U_1}{\sqrt{2}(Z_1 + Z'_2)} \\ Z'_2 &= R'_2 + jX'_2 = \frac{Z_{2s}Z_m}{Z_{2s} + Z_m} \end{aligned} \right\} \quad (14)$$

- (2) Torque:

$$T = \frac{P_e}{\Omega_s} = \frac{3I_2^2 R'_{2s}}{\Omega_s} \quad (15)$$

- (3) Efficiency:

$$\eta = 1 - \frac{\sum p}{P_1} = 1 - \frac{\sqrt{3}(I_1^2 R_1 + sI_2^2 R'_{2s})}{U_1 I_1} \quad (16)$$

- (4) Power factor:

$$\cos \phi = \frac{R}{|Z|} = \frac{R_1 + R'_2}{|Z_1 + Z'_2|} \quad (17)$$

where Z_1 , Z_{2s} , and Z_m are stator, equivalent rotor, and excitation impedances, respectively; P_e is the electromagnetic power and Ω_s is the synchronous angular velocity.

The analytical results are compared with FEM results, as shown in Figure 12. Tables 3 and 4 present the data and errors.

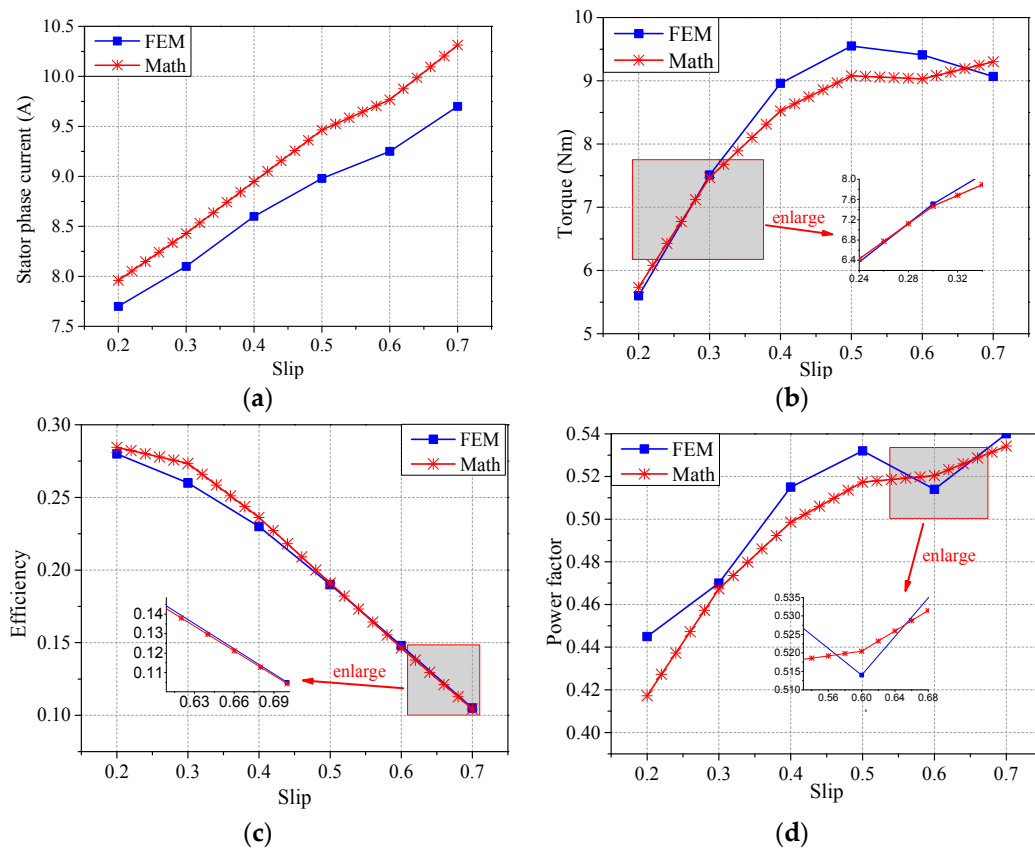


Figure 12. Characteristics of the rotary part: (a) Stator phase current; (b) Output torque; (c) Efficiency; (d) Power factor.

Table 3. Stator phase current and output torque.

Slip	Stator Phase Current (A)			Output Toque (Nm)		
	FEM	Math	Error	FEM	Math	Error
0.2	7.70	7.96	3.38%	5.62	5.73	1.96%
0.3	8.04	8.43	4.07%	7.51	7.47	0.53%
0.4	8.61	8.95	4.07%	8.96	8.53	4.80%
0.5	8.96	9.46	5.35%	9.55	9.08	4.92%
0.6	9.26	9.77	5.51%	9.41	9.03	4.04%
0.7	9.70	10.3	6.19%	9.07	9.30	2.54%

Table 4. Efficiency and power factor.

Slip	Efficiency			Power factor		
	FEM	Math	Error	FEM	Math	Error
0.2	0.28	0.284	1.43%	0.445	0.417	6.29%
0.3	0.26	0.273	5.00%	0.470	0.467	0.64%
0.4	0.23	0.236	2.61%	0.515	0.499	3.11%
0.5	0.19	0.191	0.53%	0.532	0.517	2.82%
0.6	0.15	0.146	2.67%	0.514	0.520	0.12%
0.7	0.10	0.104	4.00%	0.540	0.534	1.11%

In comparison, the curve of each parameter obtained by ECM has the same trend as the simulation curve. A close agreement exists between the analytical and simulation values. The values of the stator phase current calculated by ECM are bigger than the ones obtained by FEM and the errors are 3.38%–6.2%. For output torque, the calculation results are less than the simulation ones mostly and the calculation curve has a dent as $s = 0.6$. The errors between analytical and simulation values are $\leq 5\%$. As shown in Figure 12c, the values of efficiency calculated by ECM seem to be in good agreement with that from FEM and the errors are 0.53%–5.33%. Figure 12d and Table 4 show that the power factor, with errors in the range of 0.12%–6.29%, is underestimated by ECM. The errors are acceptable, so the ECM of the rotary part of 2DoFDDIM with SSR is valid.

5.2. The Linear Part

The analysis method of the linear part is the same as that of the rotary part. The analysis diagrams and expressions of the linear part can be obtained by interchanging the correlation quantities of the rotating part and that of the linear part in diagrams and expressions in Section 3, e.g., $Z_A \leftrightarrow Z_C$, $\dot{I}_{Am} \leftrightarrow \dot{I}_{Cm}$, $I_A \leftrightarrow I_C$, $R_A \leftrightarrow R_C$, $X_A \leftrightarrow X_C$, etc. The characteristics of the linear part are calculated and compared with simulation results, as shown in Figure 13, Tables 5 and 6.

The comparison between calculation and simulation shows that the calculation results are in good agreement with the simulation results and all of the errors are less than 8.2%. The errors are accepted. Hence, the proposed ECM is applicable to the linear part of the 2DoFDDIM with SSR. The values of stator phase current, efficiency and power factor calculated by ECM are bigger than the ones obtained by FEM. This phenomenon is caused by ignoring the influence of the edge effect and the impedance of the rotor core. For the force curves in Figure 13c, the curves obtained by calculation and simulation have the same trend. The calculation result is less than the simulation one when the slip is small ($0.2 < s < 0.5$). However, the calculation value is the bigger one when the slip is large ($0.6 < s < 0.7$).

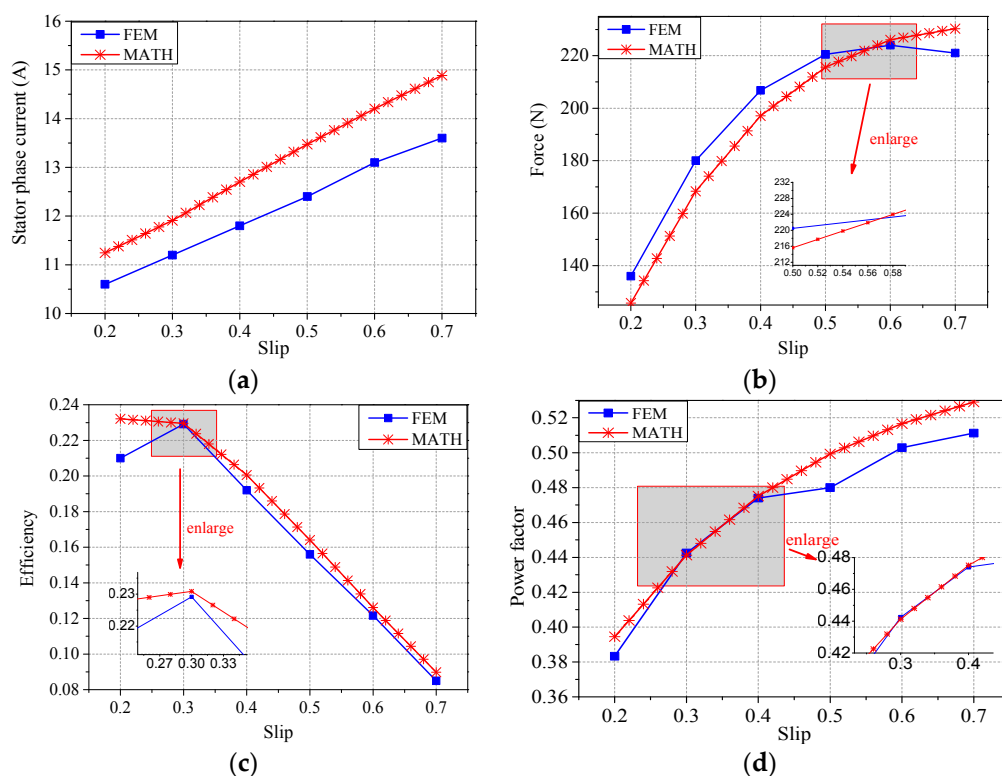


Figure 13. Characteristics of the linear part: (a) Stator phase current; (b) Force; (c) Efficiency; (d) Power factor.

Table 5. Stator phase current and force.

Slip	Stator Phase Current (A)			Output Torque (N)		
	FEM	Math	Error	FEM	Math	Error
s						
0.2	11.2	10.6	5.35%	136	125.7	7.57%
0.3	11.9	11.2	5.88%	180	168.3	6.50%
0.4	12.7	11.8	7.09%	207	197.1	4.78%
0.5	13.5	12.4	8.15%	220	215.6	2.00%
0.6	14.2	13.1	7.75%	224	226.1	0.94%
0.7	14.9	13.8	7.38%	221	230.3	4.21%

Table 6. Efficiency and power factor.

Slip	Efficiency			Power Factor		
	FEM	Math	Error	FEM	Math	Error
s						
0.2	0.219	0.232	5.94%	0.383	0.395	2.53%
0.3	0.229	0.230	0.44%	0.442	0.441	0.23%
0.4	0.192	0.200	4.17%	0.474	0.475	0.21%
0.5	0.156	0.164	5.13%	0.480	0.499	3.96%
0.6	0.122	0.126	3.28%	0.503	0.517	2.78%
0.7	0.085	0.090	5.88%	0.511	0.529	3.52%

5.3. Error Analysis

The reasons for the errors are as follows:

- (1) The influences of curvature and edge effect on the equivalent rotor impedance are neglected in ECM. Hence, the calculation values of stator phase current are less than ones obtained by FEM as shown in Figures 12a and 13a.
- (2) According to Figure 5 and Equations (15) and (17), each equivalent circuit parameter will affect the currents, leading to variation of the analytical results of torque and power factor. During the calculation of rotor parameters, the rotor core impedance is assumed to be infinite. Neglecting the influence of rotor core impedance causes the calculation result of equivalent rotor impedance to be larger than the actual value. Although the saturation effect is considered in the calculation of excitation reactance, the rotor core relative permeability is determined by experience and the excitation reactance is not accurate enough. Thus, there are errors between the analytical and simulation values of the torque and power factor, as shown in Figures 12b,d and 13b,d.
- (3) The phenomenon that the calculation values of efficiency are bigger than the simulation values is caused by ignoring the influences of harmonic effect and rotor core in ECM.

6. Conclusions

This study proposes a modified ECM to calculate the characteristics of the 2DoFDDIM with SSR from the perspective of a single-degree-of-freedom motor. The correction coefficient is used to consider the influence of the arc-shaped stator structure. The characteristics of the rotary and linear parts (i.e., stator phase current, output torque/force, efficiency, and power factor) under different slips are computed and compared with those found by FEM. The comparison shows that the analytical values are in good agreement with the simulation values. The errors, which are <8.2%, are acceptable. So, we can draw the conclusion that the modified ECM presented in this paper is reasonable and it provides reference for calculating the parameters of the induction motor with SSR.

Author Contributions: Data curation, W.W. and L.D.; Formal analysis, W.W.; Funding acquisition, J.S.; Methodology, H.F. and Z.C.; Project administration, L.D.; Software, H.F.; Writing—original draft, H.F., J.S. and W.W.; Writing—review & editing, H.F.

Funding: This work is supported by National Natural Science Foundation of China under grant 51777060 and 51277054.

Conflicts of Interest: The authors declare no conflict of interest.

References

1. Si, J.K.; Xie, L.J.; Hang, J.B. Mathematical Model of Two-Degree-of-Freedom Direct Drive Induction Motor Considering Coupling Effect. *J. Electr. Eng. Technol.* **2017**, *12*, 1227–1234. [[CrossRef](#)]
2. Si, J.K.; Xie, L.J.; Cao, W.P. Performance analysis of the 2DoF direct drive induction motor applying composite multilayer method. *IET Electr. Power Appl.* **2017**, *11*, 524–531. [[CrossRef](#)]
3. Si, J.K.; Feng, H.C.; Ai, L.W. Design and Analysis of a 2-DOF Split-Stator Induction Motor. *IEEE Trans. Energy Convers.* **2015**, *30*, 1200–1208. [[CrossRef](#)]
4. Si, J.K.; Ai, L.W.; Xie, L.J. Analysis on Electro-Magnetic Field and Performance Calculation of 2-DOF Direct Drive Induction Motor. *Trans. China Electrotech. Soc.* **2015**, *14*, 153–160.
5. Si, J.K.; Han, J.B.; Si, M. Optimization and characteristic analysis of 2-DOF direct drive induction motor. *Electr. Mach. Control* **2015**, *19*, 75–82.
6. Ho, S.L.; Niu, S.X.; Fu, W.N. A Novel Solid-Rotor Induction Motor with Skewed Slits in Radial and Axial Directions and Its Performance Analysis Using Finite Element Method. *IEEE Trans. Appl. Supercond.* **2010**, *20*, 1089–1092. [[CrossRef](#)]
7. Huang, Z.G.; Wang, S.M.; Sun, Y.G. Equivalent-circuit Parameter Calculations and Performance Analysis of Slit Solid Rotor Asynchronous Machines. *Proc. CSEE* **2017**, *37*, 1208–1215.
8. Kluszczynski, K.; Szczygie, M. How to convert a factory-manufactured induction motor into rotary-linear motor Part 1 Constructional issues. In Proceedings of the 15th International Workshop on Research and Education in Mechatronics (REM), Elgouna, Egypt, 9–11 September 2014.
9. Wang, P.X.; Si, J.K.; Feng, H.C. Mover design and characteristics analysis of 2DoFDDIM. *IET Electr. Power Appl.* **2018**, *12*, 373–378. [[CrossRef](#)]
10. Tang, Y.M. *Electric Machinery Fundamentals*, 4th ed.; China Machine Press: Beijing, China, 2011. (In Chinese)
11. Boglietti, A.; Cavagnino, A.; Lazzari, M. Computational Algorithms for Induction Motor Equivalent Circuit Parameter Determination—Part II: Skin Effect and Magnetizing Characteristics. *IEEE Trans. Ind. Electron.* **2011**, *58*, 3734–3740. [[CrossRef](#)]
12. Boglietti, A.; Cavagnino, A.; Lazzari, M. Computational Algorithms for Induction-Motor Equivalent Circuit Parameter Determination—Part I: Resistances and Leakage Reactances. *IEEE Trans. Ind. Electron.* **2011**, *58*, 3723–3733. [[CrossRef](#)]
13. Boglietti, A.; Cavagnino, A.; Lazzari, M. Algorithms for the computation of the induction motor equivalent circuit parameters—Part II. In Proceedings of the 2008 34th Annual Conference of IEEE Industrial Electronics, Orlando, FL, USA, 10–13 November 2008.
14. Boglietti, A.; Cavagnino, A.; Lazzari, M. Algorithms for the computation of the induction motor equivalent circuit parameters—Part I. In Proceedings of the 2008 34th Annual Conference of IEEE Industrial Electronics, Orlando, FL, USA, 10–13 November 2008.
15. Fu, F.L.; Tang, X.G. *Asynchronous Motor Design Manual*, 2nd ed.; China Machine Press: Beijing, China, 2006.



© 2019 by the authors. Licensee MDPI, Basel, Switzerland. This article is an open access article distributed under the terms and conditions of the Creative Commons Attribution (CC BY) license (<http://creativecommons.org/licenses/by/4.0/>).